Asymmetric post-translational modifications regulate the intracellular distribution of unstimulated STAT3 dimers

Beatriz Cardoso[1#], Ricardo Letra-Vilela[1#], Catarina Silva-Almeida[1], Ana Maia Rocha[1], Fernanda Murtinheira[1], Joana Branco-Santos[1], Carmen Rodriguez[2], Vanesa Martin[2], Mariana Santa-Marta[1] and Federico Herrera[1*]

[1]Cell Structure and Dynamics Laboratory, Instituto de Tecnologia Quimica e Biologica (ITQB-NOVA), Universidade Nova de Lisboa, Oeiras, Portugal.

[2]Instituto Universitario de Oncología del Principado de Asturias (IUOPA) and Departamento de Morfología y Biología Celular, Facultad de Medicina, c/Julian Claveria, 33006 Oviedo, University of Oviedo, Spain

# Equal contribution

[*] To whom correspondence should be addressed:

Federico Herrera, PhD. Cell Structure and Dynamics Laboratory. Instituto de Tecnologia Quimica e Biologica (ITQB-NOVA). Av. da República, Estação Agronómica Nacional, 2781-901 Oeiras, Portugal. Phone: +(351) 21 446 9300; E-mail: fherrera@itqb.unl.pt

Running title: Asymmetric PTMs regulate latent STAT3 dimer localization

Key words: STAT3, bimolecular fluorescence complementation, dimerization, post-translational modifications

Abbreviations: BiFC, bimolecular fluorescence complementation; PTMs, post-translational modifications

Funding sources: FH was supported by Project LISBOA-01-0145-FEDER-007660 (Cellular Structural and Molecular Microbiology) funded by FEDER funds through COMPETE2020 - Programa Operacional Competitividade e Internacionalização (POCI) and by national funds through Fundação para a Ciência e Tecnologia (FCT, Ref. IF/00094/2013/CP1173/CT0005). This work was also supported by the Spanish Ministry of Science and Innovation (SAF2014-58468-R) and FICYT Grants (GRUPIN14-081) to CR; and by an FCT grant to MSM (Ref. VIH/SAU/0013/2011). RLV, FM, JBS and MSM were supported by fellowships from FCT (Refs. PD/BD/128163/2016, SFRH/BD/133220/2017, SFRH/BD/85275/2012 and SFRH/BPD/105635/2015, respectively). JBS was also supported by FCT/MCTES (Ref. CBQ/04612/ICL3535).

Conflicts of Interest: The authors declare no potential conflicts of interest.

Manuscript: 10 pages. Abstract, 149 words; Main text, 1526 words; 2 Figures; 3 Supplementary Figures; 1 Supplementary Table; 20 references

Abstract

Signal Transducer and Activator of Transcription 3 (STAT3) is a ubiquitous and pleiotropic transcription factor that plays essential roles in normal development, immunity, response to tissue damage and cancer. We have developed a Venus-STAT3 bimolecular fluorescence complementation (BiFC) assay that allows the visualization and study of STAT3 dimerization and protein-protein interactions in living cells. Inactivating mutations on residues susceptible to post-translational modifications (K49R, K140R, K685R, Y705F and S727A) did not alter the basal dimerization of unstimulated STAT3, but changed significantly the intracellular distribution of STAT3 dimers. Surprisingly, the distribution of specific asymmetric STAT3 dimers (i.e. the STAT3 molecules carry different mutations) was different from symmetric dimers. Our results indicate that asymmetric post-translational modifications on STAT3 dimers could constitute a new level of regulation of STAT3 signaling. This set of Venus-STAT3 BiFC constructs provides yet unexplored means to advance our understanding of STAT3 behavior and function in cancer and beyond.

54 **Introduction**

55 The Signal transducer and activator of transcription 3 (STAT3) is a conserved
56 transcription factor that plays key roles in development, immunity, response to injury
57 and cancer (1–3). STAT3 is canonically activated by phosphorylation at Y705 upon
58 stimulation with a variety of cytokines and growth factors. However, unstimulated
59 STAT3 also dimerizes, is found in the nucleus, binds to DNA and controls the
60 transcription of a specific set of genes, different from phosphorylated STAT3 (1–6).
61 Both phosphorylated and unphosphorylated STAT3 shuttle between cytoplasm and
62 nucleus, although the mechanisms may be different (7,8). Unphosphorylated STAT3
63 accumulates in the nucleus in response to cytokines and regulates transcription by
64 binding to NFkB (9). Furthermore, STAT3 can be also found in the mitochondria,
65 where it is necessary for normal activity of the electron transport chain (1,10). This
66 function is independent of its activity as a transcription factor and Y705
67 phosphorylation, but dependent on S727 phosphorylation (1,10,11). Other post-
68 translational modifications (PTMs) can regulate the behavior and function of STAT3,
69 such as acetylation at K49 or K685 (12,13) or dimethylation at K49 or K140 (14,15).
70 Although dimethylation of the K49 or K140 residues is induced by stimulation with
71 cytokines and is favored by STAT3 phosphorylation, there is basal K49 (but not K140)
72 dimethylation in unstimulated STAT3 (14), and the same happens with STAT3
73 acetylation (12,13).

74 STAT3 homodimerization and intracellular location are key events in its biological
75 functions. Three ingenious systems have been developed so far to visualize and study
76 STAT3 dimerization in living cells, based on FRET (16), BRET (6) or the homoFluoppi
77 tag (17). The FRET/BRET systems enable the visualization of both STAT3
78 homodimerization and its interaction with other proteins in real time and in a reversible
79 manner. However, they are relatively complex and difficult to adapt for high-throughput
80 experiments, and require very skilled users for sampling and analyses. The
81 homoFluoppi system is simpler but it only allows to visualize STAT3
82 homodimerization (17). Furthermore, it only allows monitorization by microscopy, as
83 there is no change in total fluorescence but in the distribution of the fluorescence within
84 the cell, in the form of punctae (17). Bimolecular Fluorescence complementation
85 (BiFC) assays also allow the analysis of protein-protein interactions in living cells (18),
86 and their particular properties make them complementary to FRET/BRET or
87 homoFluoppi systems (19). In BiFC assays, the proteins of interest are fused to two

88 non-fluorescent, complementary fragments of a fluorescent reporter (Fig. 1A). When
89 the proteins of interest dimerize, the fragments are brought together and reconstitute the
90 fluorophore, the fluorescence being proportional to the amount of dimers. Here, we
91 developed a suit of Venus-STAT3 BiFC constructs that are not only an important
92 addition to the existing STAT3 toolset, but were also successfully employed to further
93 our current understanding of the STAT3 pathway.
94

95 **Materials and Methods**

96 In order to make the Venus-STAT3 BiFC constructs, the cDNA sequence of
97 STAT3-alpha was fused to the sequence of two complementary, non-fluorescent
98 fragments of the Venus protein (Venus 1, amino acids 1-157; and Venus 2, amino acids
99 158-238)(Fig. 1A). The deletion mutants lacking the C-terminus (ΔCT) were produced
100 by PCR-mediated subcloning using full-length Venus-STAT3 BiFC constructs as
101 templates. The original lysine (K) residues on positions 49, 140 and 685 were replaced
102 by arginine (R) residues, the tyrosine (Y) residue on position 705 by phenylalanine (F)
103 and the serine (S) residue on position 727 by alanine (A)(Fig. 1A). These mutations
104 prevent the acetylation, methylation or phosphorylation of the corresponding residues
105 but preserve the basic structural function of the original amino acids. Suppl. Table I
106 shows the primers used for subcloning and mutagenesis. Detailed methods for site-
107 directed mutagenesis, cell culture and transfection, fluorescence microscopy, flow
108 cytometry and immunoblotting were described elsewhere (18). All BiFC constructs
109 were deposited in Addgene (https://www.addgene.org/). HeLa human cervix
110 adenocarcinoma cells and HEK293 human embryonic kidney cells were acquired from
111 ATCC (references CRM-CCL-2 and CRL-1573, respectively), Leukemia inhibitory
112 factor (LIF) from R&D systems (Minneapolis, USA), and Stattic from Selleckchem
113 (Houston, USA).
114

115 **Results and Discussion**

116 *Optimization of the Venus-STAT3 BiFC system*

117 Transfection of HEK293 or HeLa cells with the wild-type (WT) pair of Venus-
118 STAT3 BiFC constructs led to successful expression of the chimeric proteins V1-
119 STAT3 and V2-STAT3 (Suppl. Fig. 1), as determined by microscopy, flow cytometry
120 (Figs. 1B and 1C, Suppl. Fig. 1A-B) and immunoblotting (Suppl. Fig. 1C).

121 Fluorescence was primarily cytoplasmic in both cell lines, with low but visible nuclear
122 signal (Fig. 1C, Suppl. Fig. 1B). Incubation with Leukemia Inhibitory Factor (LIF)
123 induced STAT3 phosphorylation and translocation to the nucleus in HEK293 and HeLa
124 cells (Suppl. Fig. 1B-C), but it did not enhance STAT3 dimerization (Fig. 1B, Suppl.
125 Fig. 1D). Incubation with STAT3 inhibitor Stattic (5 μM) or removal of the C-terminus
126 containing the SH2 domain partially prevented STAT3 dimerization (Fig. 1B),
127 consistent with previous reports (16,20). On the other hand, single or double
128 Y705F/S727A phosphoresistant mutants did not decrease fluorescence (Fig. 1B). These
129 results support relevant evidence indicating that STAT3 dimerization is actually
130 independent of phosphorylation (1,2,5,8). The behavior of the Venus-STAT3 BiFC
131 system is therefore consistent with previous reports for tagged STAT3.
132 We then analyzed the intracellular location of unstimulated STAT3 homodimers
133 carrying the same inactivating mutation in both STAT3 molecules, hereafter named
134 "symmetric STAT3 dimers". We classified cells qualitatively in three categories that are
135 mutually exclusive (their sum is 100% of cells), according to the relative intensity and
136 location of the fluorescence signal (Fig. 1C-1D): 1) predominantly in the cytoplasm
137 (e.g. WT pair), 2) predominantly in the nucleus (e.g. upon LIF induction, Suppl. Fig.
138 1B), or 3) homogeneously distributed through nucleus and cytoplasm (e.g. Y705F pair).
139 We also determined the percentage of cells with mitochondrial signal, i.e. when
140 fluorescent foci co-localized with Mitotracker Red; or intracellular inclusions, i.e. when
141 fluorescent foci did not co-localize with the dye (Suppl. Fig. 2). Although changes in
142 patterns of STAT3 dimer distribution were observed in several symmetric BiFC pairs,
143 only Y705F and S727A pairs induced significant increases in the percentage of cells
144 with homogeneous nucleocytoplasmic fluorescence or inclusions, respectively (Fig.
145 1D).
146
147 *Relative contribution of STAT3 residues on the intracellular location of unstimulated*
148 *STAT3*
149 Literature on STAT3 generally assumes, explicitly or implicitly, that STAT3
150 homodimers are formed by two identical molecules. However, in a complex
151 intracellular context this is highly unlikely, as PTMs do not occur in all the pool of
152 STAT3 molecules at the same time or with the same efficiency. We made use of the
153 unique properties of our BiFC system to determine the relative contribution of residues

154 K49, K140, K685, Y705 and S727 to the dimerization and intracellular distribution of
155 STAT3 dimers.

156 We combined all possible inactivating PTM mutations with each other, but no
157 combination had a consistent effect on STAT3 dimerization as determined by flow
158 cytometry (Suppl. Fig. 3). However, the intracellular distribution of STAT3
159 homodimers was significantly altered by specific combinations of STAT3 molecules
160 (Fig. 2A). Unlike the K49R symmetric pair, K49R asymmetric combinations
161 dominantly induced an increase in cells with homogeneous nucleocytoplasmic
162 fluorescence at the expense of cytoplasmic location (Fig. 2A), similar to the Y705F
163 symmetric pair. K140R- or K685R-containing pairs showed some tendency to shift
164 cytoplasmic location towards nucleus, but only the K140R+S727A combination
165 achieved significance. This phenotype was almost identical to the Y705F+S727A
166 asymmetric pair (Fig. 2A).

167 We then pooled and analyzed all results according to the number and type of PTM
168 mutations present in the each BiFC pair. Combinations carrying any one (asymmetric)
169 or two K-R substitutions (symmetric or asymmetric) significantly increased
170 mitochondrial translocation, while decreasing the percentage of cells with STAT3
171 dimers predominantly in the cytoplasm (Fig. 2B). Asymmetric combinations of one K-R
172 substitution and one phosphoresistant mutant also increased nuclear translocation, but
173 only 2xK-R combinations increased homogeneous nucleocytoplasmic distribution.
174 Combinations carrying any two phosphoresistant mutations (symmetric or asymmetric)
175 had no significant effect on cellular distribution of STAT3 homodimers (Fig. 2B).
176 These results indicate that specific asymmetric PTMs on STAT3 dimers can prevent
177 their nuclear import/export. This was later confirmed by pooling the data according to
178 whether the STAT3 pair was symmetric or asymmetric in their PTM mutations (Fig.
179 2C). We found that asymmetric –but not symmetric– PTM mutant combinations clearly
180 increased nucleocytoplasmic or nuclear distribution at the expense of decreasing
181 cytoplasmic localization of STAT3 homodimers. Asymmetric combinations were also
182 sufficient to produce an increase in mitochondrial localization of STAT3 dimers (Fig.
183 1C).

184 BiFC is complementary to FRET/BRET and homoFluoppi approaches. It is simpler
185 than FRET/BRET and easier to adapt to high-throughput settings. Unlike homoFluoppi,
186 it allows monitorization by flow cytometry of both STAT3 homodimerization and
187 interactions with other proteins (19). On the other hand, BiFC has lower time resolution

188 and signal-to-noise ratio (6,16,17), and the reconstitution of the fluorophore is
189 irreversible, preventing the visualization of the dissociation of STAT3 dimer (19), but
190 we have practically demonstrated its potential in the present study. Our results indicate
191 that asymmetric PTMs could constitute a new level of regulation of STAT3 behavior
192 and function. Given the essential roles of STAT3 in development, immunity, tissue
193 stress and cancer, such finding could have highly relevant implications for the
194 diagnosis, treatment and understanding of a wide spectrum of human pathologies
195 beyond cancer.
196

197 **Acknowledgements**

198 The authors thank the Advanced Imaging Unit from Gulbenkian Science Institute for
199 support with bioimaging and flow cytometry.
200

201 **References**

202 1. Srivastava J, DiGiovanni J. Non-canonical Stat3 signaling in cancer. Mol Carcinog.
203 2016 Dec;55(12):1889–98.
204 2. Yang J, Chatterjee-Kishore M, Staugaitis SM, Nguyen H, Schlessinger K, Levy DE,
205 et al. Novel roles of unphosphorylated STAT3 in oncogenesis and transcriptional
206 regulation. Cancer Res. 2005 Feb 1;65(3):939-47.
207 3. Rodrigues BR, Queiroz-Hazarbassanov N, Lopes MH, Bleggi-Torres LF, Suzuki S,
208 Cunha IW, et al. Nuclear unphosphorylated STAT3 correlates with a worse
209 prognosis in human glioblastoma. Pathol - Res Pract. 2016 Jun;212(6):517–23.
210 4. Dasgupta M, Unal H, Willard B, Yang J, Karnik SS, Stark GR. Critical Role for
211 Lysine 685 in Gene Expression Mediated by Transcription Factor
212 Unphosphorylated STAT3. J Biol Chem. 2014 Oct;289(44):30763–71.
213 5. Yang J, Stark GR. Roles of unphosphorylated STATs in signaling. Cell Res. 2008
214 Apr;18(4):443-51.
215 6. Schröder M, Kroeger KM, Volk HD, Eidne KA, Grütz G. Preassociation of
216 nonactivated STAT3 molecules demonstrated in living cells using
217 bioluminescence resonance energy transfer : a new model of STAT activation? J
218 Leukoc Biol. 2004 May;75(5):792-7.
219 7. Liu L, McBride KM, Reich NC. STAT3 nuclear import is independent of tyrosine
220 phosphorylation and mediated by importin- 3. Proc Natl Acad Sci U S A. 2005
221 Jun 7;102(23):8150-5.

222 8. Cimica V, Chen HC, Iyer JK, Reich NC. Dynamics of the STAT3 transcription
223 factor: Nuclear import dependent on ran and importin-β1. PLoS One.
224 2011;6(5):e20188.
225 9. Yang J, Liao X, Agarwal MK, Barnes L, Auron PE, Stark GR. Unphosphorylated
226 STAT3 accumulates in response to IL-6 and activates transcription by binding to
227 NF B. Genes Dev. 2007 Jun;21(11):1396–408.
228 10. Wegrzyn J, Potla R, Chwae YJ, Sepuri NBV, Zhang Q, Koeck T, et al. Function of
229 mitochondrial Stat3 in cellular respiration. Science. 2009 Feb 6;323(5915):793-7.
230 11. Zhang Q, Raje V, Yakovlev VA, Yacoub A, Szczepanek K, Meier J, et al.
231 Mitochondrial localized Stat3 promotes breast cancer growth via phosphorylation
232 of serine 727. J Biol Chem. 2013 Oct 25;288(43):31280-8.
233 12. Kang HJ, Yi YW, Hou S-J, Kim HJ, Kong Y, Bae I, et al. Disruption of STAT3-
234 DNMT1 interaction by SH-I-14 induces re-expression of tumor suppressor genes
235 and inhibits growth of triple-negative breast tumor. Oncotarget. 2015 May
236 9;8(48):83457-83468.
237 13. Ray S, Boldogh I, Brasier AR. STAT3 NH2-terminal acetylation is activated by the
238 hepatic acute-phase response and required for IL-6 induction of angiotensinogen.
239 Gastroenterology. 2005 Nov;129(5):1616-32.
240 14. Dasgupta M, Dermawan JKT, Willard B, Stark GR. STAT3-driven transcription
241 depends upon the dimethylation of K49 by EZH2. Proc Natl Acad Sci. 2015
242 Mar;112(13):3985–90.
243 15. Yang J, Huang J, Dasgupta M, Sears N, Miyagi M, Wang B, et al. Reversible
244 methylation of promoter-bound STAT3 by histone-modifying enzymes. Proc
245 Natl Acad Sci U S A. 2010 Dec 14;107(50):21499-504.
246 16. Domoszlai T, Martincuks A, Fahrenkamp D, Schmitz-Van de Leur H, Kuster A,
247 Muller-Newen G. Consequences of the disease-related L78R mutation for
248 dimerization and activity of STAT3. J Cell Sci. 2014 May 1;127(Pt 9):1899-910.
249 17. Okada Y, Watanabe T, Shoji T, Taguchi K, Ogo N, Asai A. Visualization and
250 quantification of dynamic STAT3 homodimerization in living cells using
251 homoFluoppi. Sci Rep. 2018 Feb 5;8(1):2385.
252 18. Branco-Santos J, Herrera F, Poças GM, Pires-Afonso Y, Giorgini F, Domingos PM,
253 et al. Protein phosphatase 1 regulates huntingtin exon 1 aggregation and toxicity.
254 Hum Mol Genet. 2017 Oct 1;26(19):3763-3775.
255 19. Herrera F, Gonalves S, Outeiro TF. Imaging protein oligomerization in

256 neurodegeneration using bimolecular fluorescence complementation. Methods
257 Enzymol. 2012;506:157-74.
258 20. Schust J, Sperl B, Hollis A, Mayer TU, Berg T. Stattic: A Small-Molecule Inhibitor
259 of STAT3 Activation and Dimerization. Chem Biol. 2006 Nov;13(11):1235-42.
260

261 **Figure Legends**

262 **Figure 1. A Venus-STAT3 BiFC system allows the visualization and study of**
263 **STAT3 homodimers in living cells.** A, Venus BiFC fragments constituted by amino
264 acids 1-158 (Venus 1, V1) and 159-238 (Venus 2, V2) were fused to the N-terminus of
265 the STAT3 sequence in two independent constructs. When two STAT3 molecules
266 carrying complementary Venus fragments dimerize, the Venus protein becomes
267 functional and emits fluorescence, which is proportional to the amount of STAT3
268 homodimers. K49, K140, K685, Y705 and S727 residues can be post-translationally
269 modified, and were inactivated in both V1- and V2-STAT3 constructs by site-directed
270 mutagenesis. Additionally, the C-terminus was removed in a V2-STAT3 BiFC construct
271 in order to confirm that this region was involved in STAT3 homodimerization. B, Wild-
272 type Venus-STAT3 constructs produced fluorescence in HeLa cells, and it was
273 monitored by flow cytometry 24 hours after transfection with BiFC constructs.
274 Incubation with Leukemia Inhibitory Factor (100 ng/ml) for 2 hours in the absence of
275 serum or the presence of single or double phosphoresistant mutations in BiFC pairs did
276 not produced significant changes in the percentage of fluorescent cells. On the other
277 hand, incubation with the STAT3 inhibitor Stattic (5 μM) for 24 hours or removal of the
278 C-terminus, containing the SH2 region involved in STAT3 homodimerization,
279 significantly decreased the percentage of fluorescent cells ($n=3$, $p<0.05$). Results were
280 normalized versus the Wild-type STAT3 pair (100%). C, microscopy pictures of
281 representative cell phenotypes in the different symmetric combinations of BiFC Venus-
282 STAT3 constructs (Incl, inclusions; Scale bar, 20μm). D, Percentage of cells displaying
283 fluorescence predominantly in the Nucleus (black bar), predominantly in the Cytosol
284 (white bar), homogeneously distributed in cytoplasm and nucleus (nucleocytoplasmic,
285 grey bar), in the mitochondria or in non-mitochondrial inclusions. Data are shown as the
286 average ± Standard Error (SEM) of $n=12$ (Wild-type, WT) or $n=3$ (rest of
287 combinations) independent experiments. Statistical analysis was carried out by means of
288 a One-way ANOVA followed by a Bonferroni test corrected for multiple comparisons.
289 *, significant vs the symmetric Wild-type STAT3 pair, $p<0.05$.

290

291 **Figure 2. Asymmetric STAT3 PTMs regulate intracellular distribution of STAT3**
292 **homodimers.** A, Intracellular distribution of fluorescence in asymmetric combinations
293 of Venus-STAT3 BiFC constructs (and the WT symmetric pair as reference). Data are
294 shown as the average of n=12 (Wild-type, WT) or n=3 (rest of combinations)
295 independent experiments. Errors represent the Standard Error. Statistical analysis was
296 carried out by means of a One-way ANOVA followed by a Bonferroni test corrected for
297 multiple comparisons. *, significant vs the symmetric Wild-type STAT3 pair, *, $p<0.05$,
298 ** $p<0.01$. B-C, The same original data, but pooled according to the number and nature
299 of substitutions (B) or the symmetry or asymmetry of substitutions (C) in the STAT3
300 homodimer, and represented as box plots. The limits of the boxes represent the smallest
301 and largest values, the straight line represents the median, the dashed line represents the
302 average, and the dotted line represents the average for wild-type STAT3 pair. Statistical
303 analysis was carried out on the Average ± Standard Error of each pool of data by means
304 of a One-way ANOVA followed by a Bonferroni test corrected for multiple
305 comparisons. *, significant vs the symmetric Wild-type STAT3 pair, *, $p<0.05$, **
306 $p<0.01$; #, significant vs 2xYF/SA substitution (in B) or the symmetric mutant pairs (in
307 C), #, $p<0.05$, ##, $p<0.01$.

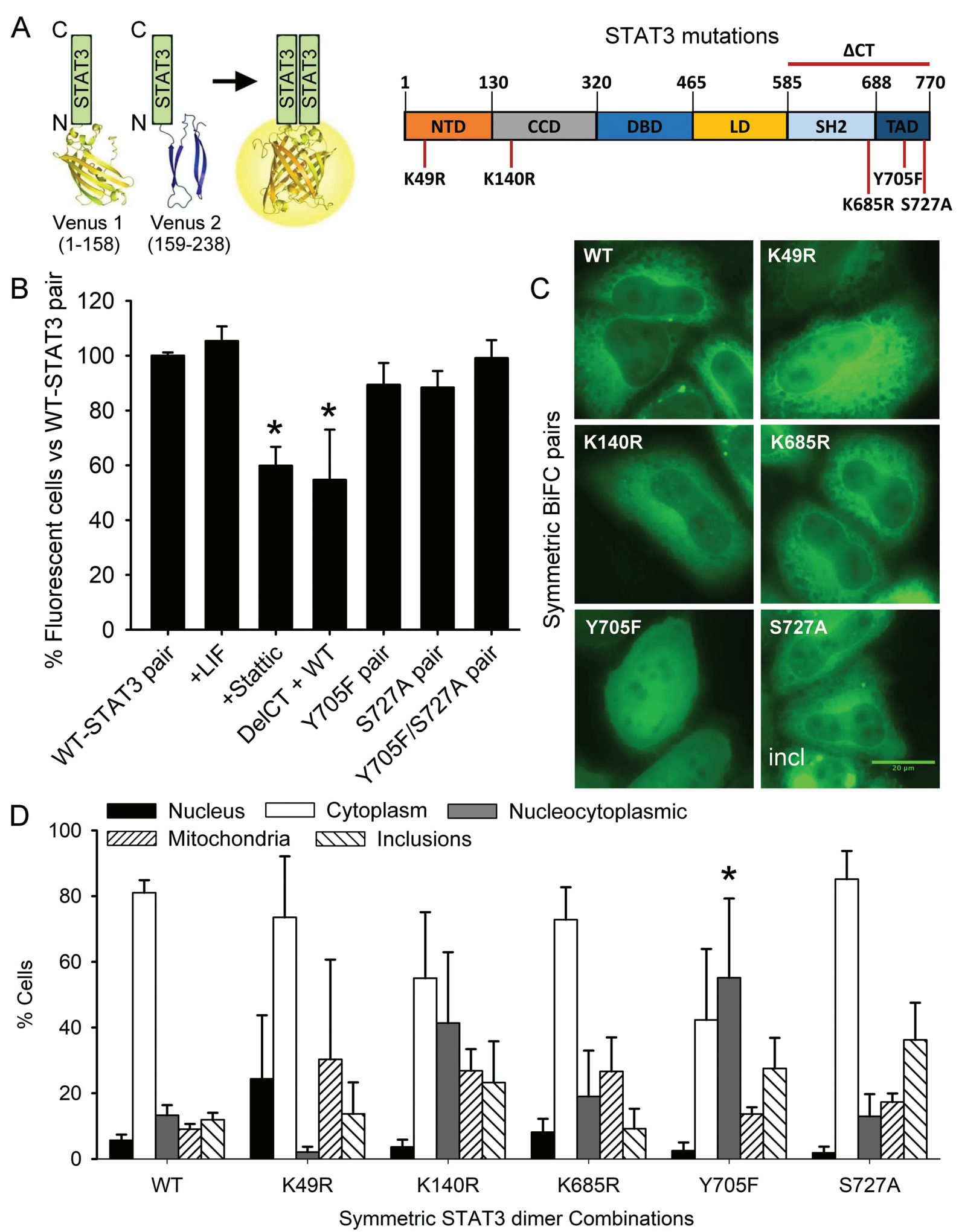
A
C
STAT3
N
Venus 1
(1-158)
Venus 2
(159-238)
STAT3 mutations
ΔCT
1
130
320
465
585
688
770
NTD
CCD
DBD
LD
SH2
TAD
K49R
K140R
Y705F
K685R
S727A
B
% Fluorescent cells vs WT-STAT3 pair
WT-STAT3 pair
+LIF
+Stattic
DelCT + WT
Y705F pair
S727A pair
Y705F/S727A pair
C
Symmetric BiFC pairs
WT
K49R
K140R
K685R
Y705F
S727A
incl
20 µm
D
Nucleus
Cytoplasm
Nucleocytoplasmic
Mitochondria
Inclusions
% Cells
WT
K49R
K140R
K685R
Y705F
S727A
Symmetric STAT3 dimer Combinations

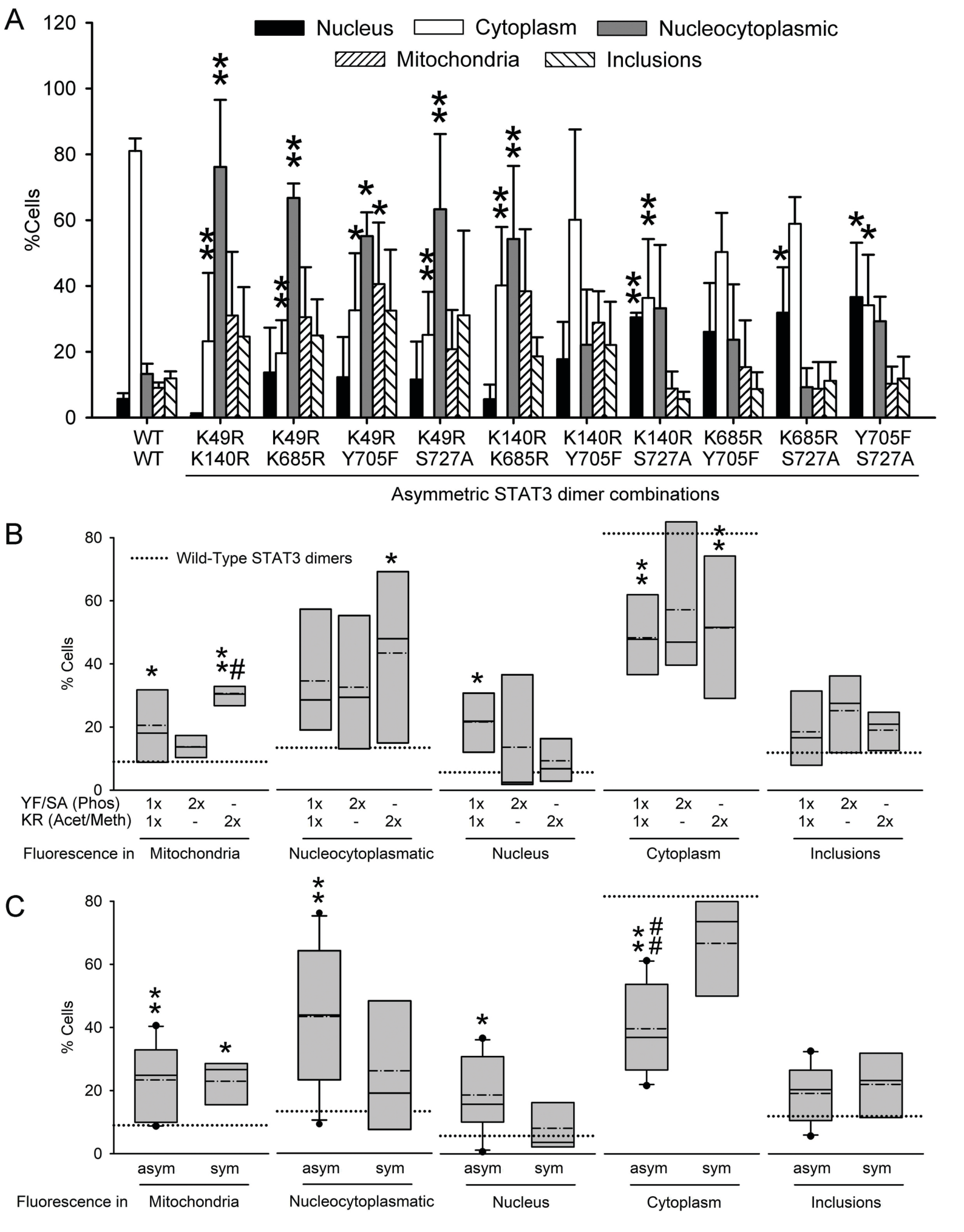
A
Nucleus
Cytoplasm
Nucleocytoplasmic
Mitochondria
Inclusions
%Cells
120
100
80
60
40
20
0
WT WT
K49R K140R
K49R K685R
K49R Y705F
K49R S727A
K140R K685R
K140R Y705F
K140R S727A
K685R Y705F
K685R S727A
Y705F S727A
Asymmetric STAT3 dimer combinations
B
Wild-Type STAT3 dimers
% Cells
80
60
40
20
0
YF/SA (Phos) 1x 2x -
KR (Acet/Meth) 1x - 2x
Fluorescence in Mitochondria
Nucleocytoplasmatic
Nucleus
Cytoplasm
Inclusions
C
% Cells
80
60
40
20
0
asym sym
Fluorescence in Mitochondria
Nucleocytoplasmatic
Nucleus
Cytoplasm
Inclusions